The DOI for this manuscript is doi:
10.1175/2009JTECHO711.1

Identifying and Estimating Biases between XBT and Argo Observations Using Satellite Altimetry

Pedro N. DiNezio.

Cooperative Institute for Marine and Atmospheric Studies

University of Miami

4600 Rickenbacker Causeway

Miami, FL 33149

Gustavo J. Goni

National Oceanic and Atmospheric Administration

Atlantic Oceanographic and Meteorological Laboratory

4301 Rickenbacker Causeway

Miami, FL 33149

Abstract

A methodology is developed to identify and estimate systematic biases between eXpendable BathyThermograph (XBT) and Argo observations using satellite altimetry. Pseudo-climatological fields of isotherm depth are computed by least squares adjustment of in–situ XBT and Argo data to altimetry–derived sea height anomaly (SHA) data. In regions where the correlations between isotherm depth and SHA are high, this method reduces sampling biases in the *in situ* observations by taking advantage of the high temporal and spatial resolution of satellite observations. In this study we consider temperature profiles from *deep* XBTs corrected for a bias identified and adopted during the 1990s. Our analysis shows that the pseudo-climatological isotherm depths derived from these corrected XBTs are predominantly deeper than the Argo-derived estimates during the 2000–2007 period. The XBT minus Argo differences increase with depth consistent with hypothesized problems in the XBT fall rate equations. The depth-dependent XBT minus Argo differences suggest a global positive bias of 3% of the XBT depths. The fact that this 3% error is robust among the different ocean basins provides evidence for changes in the instrumentation, such as changes in the terminal velocity of the XBTs. The value of this error is about the inverse of the correction to the XBT fall-rate equation (FRE) implemented in 1995, suggesting that this correction, while adequate during the 1990s, is no longer appropriate, and could be the source of the 3% error. This result suggests that for 2000-2007, the XBT dataset can be brought to consistency with Argo by using the original FRE coefficients without the 1995 correction.

Introduction

eXpendable BathyThermographs (XBT) are widely used to observe the thermal structure of the upper ocean and constitute a large fraction of the archived ocean thermal data during the 70s, 80s and 90s. Until the advent of the Argo array, XBTs dominated the global ocean thermal observations, currently; XBTs represent approximately 25% of current ocean temperature profile observations, being a valuable complement for the Argo array. Unlike Argo observations, XBTs determine the depth of the temperature observations indirectly. The time in seconds elapsed since the XBT hits the ocean surface is converted into depth, z_{xbt}, using a fall-rate equation (FRE):

$$z_{xbt} = bt - at^2 \quad (1),$$

where the a and b coefficients are empirical constants related to the physics of the probe descent.

This FRE results from a simple dynamical model of the descent of the XBT with the net buoyant force being balanced by hydrodynamic drag proportional to the square of the probe speed (Green 1984; Hallock and Teague 1992). The linear term bt in (1) results from this balance neglecting the acceleration of the probe d^2z/dt^2. As a result the fall speed is virtually equal to the terminal velocity, a reasonable assumption for depths larger than 10 m. The b coefficient represents the value of this terminal velocity and is, to first-order, determined by the drag coefficient and the mass of the probe in the water. The deceleration term $-at^2$ accounts for the both the reduction of probe mass as the wire pays out and the increasing drag with depth, where the later is more important. The depth dependence of the fall-rate due to changes in sea water density is one order of magnitude smaller than the temperature dependence of the drag or the mass loss due to wire payout (Green 1984).

The bulk of XBT temperature profiles are collected using probes manufactured by Sippican Incorporated (now Lockheed Martin Sippican, hereinafter Sippican). Even though these coefficients are based on physical parameters of the probe (Green 1984), they are empirically determined by the manufacturer with standard values for b = 6.472 m s^{-1} and $a = 216\times10^{-5}$ m s^{-2}. The processes involved in the descent of an XBT probe are certainly more complex than the first-order dynamics implied in equation (1). As a result, the determination of the XBT depth is the most important source of error in XBT temperature profiles with reported values of 17 m, (McDowell 1977; Seaver and Kuleshov 1982) and 19 m (Fedorov et al. 1978) at 750 m depths. Systematic errors in the computed XBT depths have been identified since the mid 1970s: Comparison studies between simultaneous XBTs and Conductivity Temperature Depth (CTD) casts found a small positive bias above the thermocline and a much larger negative bias for depths below (Fedorov 1978; Flierl and Robinson 1977; McDowell 1977; Seaver and Kuleshov 1982). Evidence of surface offsets associated with initial transients has also been found (e.g. Singer 1990), pointing at the limitations of (1) in the determination of XBT depths. Nonetheless, XBT temperature profiles have been shown to be accurate enough to characterize mesoscale phenomena (Seaver and Kuleshov 1982; Flierl and Robinson 1977).

It was not until the 1990s when the impact of these systematic errors on climate applications was recognized. Sippican adopted a correction factor after a comprehensive analysis of research-quality CTD and XBT data by Hanawa et al. (1995 - hereinafter H95). This study showed that the Sippican coefficients in the FRE resulted in depths that were too shallow, producing a cold temperature bias in most of the water column. A stretching factor f_{H95} = 1.0336 was recommended to correct this bias, and later applied to the Sippican original FRE as follows:

$$z_{H95} = f_{H95}\left(bt - at^2\right). \qquad (2)$$

Recent studies suggest time-varying biases between XBT and CTD observations that are consistent with changes in the *b* coefficient, i.e. the probe's terminal velocity (Gouretski and Koltermann 2007; Wijffels et al. 2008; Ishii and Kimoto 2009). The time-varying errors found by these studies represent up to 10% changes in the *b* coefficient of the FRE, leading to commensurate changes in z_{xbt}. The implied changes in the FRE exceed the 2% error specified by Sippican and are likely to be responsible for spurious decadal signals in global mean heat storage time series (Wijffels et al. 2008; Levitus et al. 2009).

Starting in 2000, the rapidly expanding Argo array (Gould et al. 2004) provides global and highly quality controlled ocean temperature and salinity data with CTD accuracy. Nonetheless, XBT profiles make up to 25% of the current global temperature profile observations during the period of study. Therefore, assessing and correcting this bias is key to monitoring changes of global ocean heat content. Moreover, systematic biases between observing systems with disparate quality capabilities, such as Argo and XBTs, can also introduce spurious climatic signals in heat storage as the ratio of the number of observations collected with each platform changes (e.g. Willis et al. 2009). Argo and CTD profiles also have uncertainties in the determination of pressure/depth. For instance, profiles from Argo floats are often corrected for drifts in the pressure sensor (http://www.argo.ucsd.edu/Acpres_drift_apex.html). Most of the Argo pressure drifts are less than 2 db with very rare cases as large as 10 db. These large drifts are unlikely to have a global impact compared with the hypothesized XBT bias, which if detected, should exhibit a global extent. Moreover, the magnitude of the hypothesized XBT bias, about 20 m at 700 m depth (e.g. Wijffels et al. 2008, Figure 6), is substantially larger than the Argo drifts in addition to having very different depth dependence. Ideally, XBT data should be evaluated against CTD data in order to obtain an absolute correction (e.g. Hanawa et al. 1995). However, the sparse coverage provided by CTDs during the 2000-2007 period does not permit a global comparison. For these reasons, in this study we evaluate XBTs relative to Argo data. This should be kept in mind if the correction derived here is applied to XBT data.

Most intercomparisons have focused on localized concurrent CTD and XBT casts, which have limited temporal and spatial scope. On the other hand, very few studies have analyzed the spatial dependence of these errors (e.g. Schmid 2005; Wijffels et al. 2008). In this study we use temperature profiles obtained from XBT and Argo combined with satellite altimetry observations to investigate the spatial dependence of potential XBT errors globally. Simultaneously, a methodology is developed to estimate the uncertainty of these errors. This methodology takes advantage of the high correlation between satellite altimeter sea height observations and the thermal structure of the upper ocean to reduce uncertainty associated with sampling by *in situ* observations. This methodology is shown to produce statistically significant (1-sigma) estimates of the XBT bias over relatively short periods compared with conventional climatologies, thus becoming a viable procedure to correct future XBT observations on an operational basis. Furthermore, in this study we characterize the spatial extent of this bias[1] and provide more evidence for a FRE problem.

Data

Temperature profiles obtained from XBTs, profiling floats, and CTD casts are used in this study. The XBT data are obtained from Global Temperature-Salinity Profile Program (GTSPP; http://www.nodc.noaa.gov/GTSPP). The profiling float data are available from the GTSPP and from the Argo Global Data Assembly Centers (GDAC; http://www.usgodae.org/argo/argo.html and http://www.coriolis.eu.org/cdc/argo.htm). CTD data are also obtained from the GTSPP. Temperature profiles in the GTSPP and GDACs are typically quality controlled with different standards. All profiles analyzed here, including XBTs, are quality controlled following an additional procedure based on

[1] The term bias and error used indistinguishably throughout this paper to refer to those errors that are systematic.

the standard procedures that are approved by the international Argo data management team consisting of removal of duplicates, spike detection, pressure increasing test, and a vertical gradient test (Schmid 2005). In addition, the profiles were compared with climatology (Conkright et al. 2002). For the Argo data, only pressure and temperature values with quality control flags equal to 1 are used in addition to "adjusted" fields when available. Since 50% of the Argo profiles collected during the 2000-2007 are available in delayed-mode, real-time profiles were used to complete the Argo data. After the additional quality control and duplicates removal are performed, the majority (85%) of the non-XBT profiles used in our study are profiling floats obtained from the Argo GDAC. The remaining profiles are profiling float profiles obtained from the GTSPP (5%) and CTDs (10%). Approximately 120.000 XBT temperature profiles and 380.000 Argo and CTD temperature profiles that passed the quality control were included in this study.

All XBT-derived profiles analyzed here correspond to "deep" XBTs, such as Sippican models T7 and DeepBlue. These XBTs are designed to reach depths of about 750 m and represent the bulk of the XBT observations since 2000. Profiles shorter than 550 m were not considered to avoid including *shallow* XBTs, which have different FRE coefficients. The transition from the original Sippican coefficients to the H95 correction has resulted in profiles submitted to the GTSPP with the original FRE during a period after the H95 correction was recommended (Wijffels et al. 2008). Some profiles were submitted to the GTSPP without any information on the coefficients used in the FRE. However, from 2000 to 2007 virtually all profiles include information indicating the FRE coefficients, with the majority including the H95 correction. In this study, we only consider XBT profiles with FRE coefficients unambiguously indicated in the profile. The H95 correction was applied whenever the metadata unambiguously indicated that it was not applied in the data submitted to the GTSPP. About 20% of the XBT profiles required this adjustment. No profiles with ambiguous FRE coefficients were found for the period of study. As a result, all XBT profiles considered in this study have the H95 FRE coefficients applied. A pressure offset has been recently found in a group of Argo profiling floats. All temperature profiles obtained by floats with this problem have not been considered in this study following the recommendation of the Argo project (http://www-argo.ucsd.edu/Acpres_offset2.html).

Altimetry-derived sea surface height observations are used in this study for two reasons: first, to avoid potential biases in climatological estimates of isotherm depth that arise from the relatively inhomogeneous sampling inherent to *in situ* hydrography; second, to reduce the uncertainty of the climatological estimates of isotherm depth in regions where the thermal structure of the upper ocean is correlated with the sea surface height. The altimetry data used here are the delayed-mode optimally interpolated gridded sea surface height (SHA) fields produced by AVISO according to the methodology of Le Traon et al. (1998), with spatial resolution of 0.25 degrees, and with temporal resolution of 1 week. The altimetric observations used to produce these gridded fields were obtained from two or three satellites throughout the period from January 2000 to December 2007. The AVISO SHA fields are anomalies computed with respect to the 1993 – 1999 mean from the direct altimetry observations. Therefore, the time-mean field for the 2000-2007 period is not necessarily zero. To apply our methodology we removed the time-mean SHA corresponding to the 2000-2007 period on every grid point. This simplifies the interpretation of the isotherm depth estimates obtained results from our methodology as climatological mean estimates.

Methods

The methodology to identify and quantify biases between XBT and Argo observations presented here consists of the following steps:

1. The climatological isotherm depths and their uncertainty are estimated from H95-corrected XBTs and from Argo profiles separately. Due to the short duration of the Argo dataset, correlations with altimetry-derived SHA fields are used to reduce the uncertainty of the isotherm depth estimates.

2. The geographical distribution of the differences between XBT minus Argo isotherm depths is analyzed. Systematic biases between the two observing systems are expected to affect the mean climatological estimates. Only differences with non-overlapping 1-sigma confidence intervals are considered.

3. The depth dependence of the XBT minus Argo differences are analyzed to confirm a problem in the XBT FRE. The depth dependent biases in the XBTs are estimated globally, and in different regions, to infer other potential sources of error than the FRE.

Potential biases in the XBT observations are explored here by comparing estimates of the mean-climatological isotherm depth derived from XBTs with estimates derived from Argo profiling-floats and CTDs. Throughout the analysis, Argo and CTD observations, are collectively referred to as Argo due to the prevalence of this platform during the period of study. Unlike XBTs, Argo and CTD casts measure the pressure at each temperature observation directly. Thus, the depth of these temperature profiles is determined with higher accuracy than the XBT FRE. For Argo and CTD profiles the pressure is converted into depth following a methodology that accounts for the variation of gravity with latitude and depth, and the effect of pressure on density (Saunders 1981). This methodology neglects the small influence of salinity and temperature on density with an error less than 0.25 m, which is at least one order of magnitude smaller than the hypothesized biases in the FRE equation we seek to identify and quantify. For these reasons, in this study we evaluate the depth of isotherms derived from XBT data relative to Argo data, since the latter are expected to have smaller systematic biases.

Several studies have shown that observations of sea surface height are strongly correlated with the thermal structure of the upper ocean (Goni et al. 1996; Gilson et al. 1998; Mayer et al. 2001; Willis et al. 2004). Based in this virtually ubiquitous relationship, we propose a methodology that combines altimetry-derived SHA fields with *in situ* temperature profiles to produce climatologies capable of quantifying potential biases in the XBT observations. The depths of the 5°C to 28°C isotherms, every 1°C, are estimated for each XBT and Argo temperature profile. The SHA fields are interpolated into the location and day of the temperature profiles using a Gaussian filter in space and linear interpolation in time. The pairs of interpolated SHA values and *in situ* isotherm depths are binned into 3°×3° bins globally, with XBT and Argo profiles separately. On each 3°×3° bin, the isotherm depth values are linearly regressed on the interpolated SHA estimating a correlation coefficient, regression gain, and a y-intercept.

Results for the depth of the 10°C and 20°C isotherms are highlighted because these isotherms lie in thermocline waters in subtropical and equatorial oceans respectively. The spatial distribution of the correlation coefficients obtained for the depth of the 10°C isotherm (h_{10}) are similar between estimates using Argo (Figure 1a) and XBT (Figure 1b) observations. High correlations ($r > 0.6$) are found in regions where this isotherm is within thermocline waters, such as in the subtropical gyres, with the exception of the South Atlantic subtropical gyre where observations are scarce. The correlation coefficients obtained for the depth of the 20°C isotherm (h_{20}) show high values in the equatorial oceans both for Argo (Figure 1c) and XBT (Figure 1d) observations. The correlation coefficients between the Argo-derived isotherm depth and altimetry-derived SHA are statistically significant over most of the global ocean with a 67% confidence level (1-sigma) based on a chi-squared distribution. The correlation coefficients between XBT-derived isotherm depth and altimetry-derived SHA are statistically significant (1-sigma) over regions covered by XBT transects, where the density of observations is largest. We assume that all observations are independent in the estimation of the statistical uncertainty. This is a reasonable assumption for the Argo profiles, which could show some correlation between successive 10-day profiles, but are generally decoupled between casts in Ekman layer. In contrast, multiple XBT casts sampling one single mesoscale feature are more common along high-density transects (Roemmich and Gilson 2001). In these cases, the uncertainty of the correlations will be underestimated. However, the conclusions presented are robust because our estimation of the depth-dependent XBT error is performed using estimates of isotherm depth resulting from regions with very high correlations (r > 0.8) with the SHA fields. We tested the robustness of our results by considering the case of three XBTs sampling the same eddy, resulting in factor of $\sqrt{3}$ increase in the confidence interval, but without impact on the estimate of the XBT minus Argo bias.

Global fields of regression gain and y-intercept are obtained by least-squares fitting of a straight line to the pairs of interpolated SHA values, η', and the *in situ* isotherm depth observations, h, on each 3°×3° bin:

$$\hat{h} = \varepsilon^{-1} \cdot \eta' + \tilde{h}, \qquad (3)$$

where $\hat{h}$ is the isotherm depth estimated by this statistical model for each altimetry-derived η' value, ε^{-1} is the regression gain, and $\tilde{h}$ is the y-intercept. For each isotherm, the regression slope, ε^{-1}, is related to the reduced gravity of a two-layer model, thus representing a measure of the local stratification. Conversely, since the time-mean value of η' at each location is zero, the y-intercept, $\tilde{h}$, represents the time-mean isotherm depth predicted by this statistical two-layer model. We refer to $\tilde{h}$ as pseudo-climatology, to distinguish it from the climatology obtained from averaging the Argo or XBT observations directly:

$$\bar{h} = \sum h_i / N \quad (4).$$

The pseudo-climatologies, $\tilde{h}$, obtained from (3) weight the *in situ* observations with the satellite-derived η' fields in a least-squares sense. This procedure avoids biases due to inhomogeneous sampling and reduces the statistical uncertainty of the pseudo-climatologies. In the following subsections we discuss these two key features of the methodology that allow identification and estimation of potential biases in the XBT observations.

a. Reduced Sampling Bias

Throughout this study we compare the parameters obtained from the regression (3) between the satellite-derived η' and h obtained from each platform. Any statistical significant difference between the regression parameters may be indicative of problems in either or both platforms. Argo floats have high accuracy in depth and temperature but may have spatial and temporal sampling problems inherent of a Lagrangian observing platform. XBTs are also prone to sampling problems, however, their most important source of error is in the determination of depth, which are much larger that errors in the temperature sensor. As discussed in the introduction, there is evidence suggesting that XBTs suffer from systematic biases associated with changes in the coefficients of the FRE (1). In regions of high correlations, the methodology proposed here reduces the sampling bias using high resolution SHA fields, allowing us to identify other systematic errors, such as those associated with the FRE. Thus, discrepancies in the regression parameters will point to problems related to XBT depth estimates.

Both climatology estimators $\tilde{h}$ and $\bar{h}$ are related through the correlation coefficient, r, and mean SHA, $\bar{\eta}'$, according to basic properties of the least-squares method (Lawson and Hanson, 1974):

$$\tilde{h} = \bar{h} - r\frac{\sigma_h}{\sigma_\eta}\bar{\eta}', \qquad (5)$$

where σ_h and σ_η are the standard deviation of the h and η' observations respectively. Note that while the time-mean η' is zero, the mean η' corresponding to the *in situ* observations, $\bar{\eta}'$, is not necessarily zero due to the inhomogeneous temporal and spatial sampling of XBT and Argo observations at each location. For instance, when *in situ* observations are predominantly collected in anti-cyclonic eddies, which are characterized by positive η' values and isotherms deeper than the background flow; the $\bar{h}$ will be biased towards large values. In this case, the $r\sigma_h/\sigma_\eta\,\bar{\eta}'$ term in (5) represents a correction to this bias. If observations are biased towards anti-cyclonic eddies, then $\bar{\eta}'$ > 0 and according to (5) the $\tilde{h}$ estimate will be lower than $\bar{h}$.

For example, 82 Argo and 36 XBT quality controlled observations are analyzed in a 3°×3° bin centered in 169°W 4°S. The mean depths of the 20°C isotherm estimated from Argo and XBTs are $\bar{h}_{20}$ = 179.4±1.3 (Argo) and $\bar{h}_{20}$ = 182.9±2.4 (XBT), where the uncertainty is given by the standard error of the sample. The 1-sigma confidence intervals overlap, therefore the two estimates are statistically indistinguishable with a 67% probability. A scatter plot of the observed isotherm depths from each platform and their corresponding η'values (Figure 2a), suggests that 66 out of 82 Argo observations were collected over positive η' values. In other words, most of the Argo observations were collected over anticyclonic features; therefore the $\bar{h}$ estimate must be deeper than that derived from XBTs, which were obtained at locations with evenly distributed positive and negative η' values. However, the $\bar{h}$ estimates do not show a significant difference, this raises an apparent contradiction that could be explained by a systematic deep bias in the XBT observations.

This apparent contradiction may be elucidated with the analysis of the results from the linear regression. The correlation coefficients are 0.6 and 0.5 for Argo and XBT, respectively. The regression gains obtained from each platform are statistically indistinguishable within 1-sigma confidence levels. On the other hand, the y-intercepts or pseudo-climatology estimates are statistically distinct within 1-sigma confidence levels, with values of $\tilde{h}_{20} = 172.1 \pm 1.4$ (Argo) and $\tilde{h}_{20} = 181.2 \pm 2.1$ (XBT). These estimates suggest that XBTs overestimate the depth of the 20°C isotherm by about 10 m. This difference between the estimates is statistically significant based on the 1-sigma confidence intervals of the y-intercept resulting from the linear regressions, $\tilde{h}$.

The previous example illustrates how in regions of high correlations, this methodology takes advantage of the homogenous sampling of satellite altimetry to correct biases in the estimates of isotherm depth. On the other hand, when the sampling is homogeneous and in the absence of systematic biases, $\bar{h}$ and $\tilde{h}$ converge to the same value. Thus, in regions with high density of observations the $\bar{h}$ and $\tilde{h}$ estimates are expected to converge. For instance, in the 3°×3° bin centered in 175°E 25°S the number of XBT and Argo observations is large and the *in situ* observations are evenly distributed between positive and negative η' values (Figure 2b). This example shows how the climatological estimates converge when the sampling is homogeneous in each platform. This is shown by the overlapping between the $\bar{h}$ and $\tilde{h}$ estimates obtained from each platform respectively (Figure 2b). However, the $\bar{h}$ and $\tilde{h}$ estimates show a difference of about 30 m between Argo and XBT, which cannot be explained as a sampling bias and could result from biases in either observing platforms.

b. Reduced Statistical Uncertainty

As already discussed in the introduction, several studies have provided evidence for a systematic bias in the XBT observations consistent with a FRE problem. Any problem in the FRE equation leading to a systematic bias in the determination of the XBT depth could be identified by analyzing the differences between climatologies $\bar{h}$, derived from XBTs and Argo. This methodology has been applied to identify XBT biases over long periods of time (Gouretski and Koltermann 2007; Wijffels et al. 2008). Argo observations do not allow the estimation of climatologies with uncertainties required to identify systematic biases with a magnitude of less than 20 m found by the previous studies mentioned in the introduction. This limitation becomes more important for characterization of the spatial extent of this bias during the relatively short 2000-2007 period. However, any systematic bias in the XBT observations could also be identified in the pseudo-climatologies $\tilde{h}$. According to the least-squares method (e.g. Lawson and

Hanson, 1974) the standard error of $\tilde{h}$ is related to the standard error of the climatological isotherm depth, $\bar{h}$, through the correlation coefficient, r:

$$S(\tilde{h}) = \sqrt{(1-r^2)\left(1+\frac{\overline{\eta'}}{\sigma_\eta}\right)} S(\bar{h}), \qquad (6)$$

where $S(\ )$ represents the standard error estimator, $\overline{\eta'}$ is the mean value of the η' observations, and σ_η is their standard deviation. This equation shows that the statistical uncertainty of the $\tilde{h}$ estimates is reduced in the limit of $\overline{\eta'} \sim 0$, which corresponds to homogenous sampling. In other words, the standard errors are related by the $\sqrt{(1-r^2)}$ factor, which is always less than 1, when the *in situ* observations are equally distributed between positive and negative values of SHA (i.e. $\overline{\eta'}$)=0. Therefore, when correlations are high and sampling is homogeneous, the uncertainty of the pseudo-climatology $\tilde{h}$, is reduced with respect to the climatological isotherm depth $\bar{h}$. This feature of the methodology becomes more important in regions where the variability of the thermal structure of the upper ocean is large because σ_h is large. To conclude, in the limit of no correlation between h and η', $\tilde{h}$ converges to $\bar{h}$ (5) and so do the standard errors (6), thus the methodology defaults to a conventional climatology.

Results

Global maps of $\tilde{h}$ are estimated for isotherms from 5°C to 28°C (every 1°C) for XBT and Argo observations separately. In this section we describe the spatial features of the pseudo-climatologies and the differences between XBT and Argo estimates, focusing on the 10°C and 20°C isotherms. The estimates of $\tilde{h}_{10}$ obtained from XBTs and Argo show similar spatial patterns consistent with large scales ocean features, such as gyres, currents, and fronts (Figure 3). For example, the pseudo-climatologies capture the deepening of the 10°C isotherm towards the centers of subtropical gyres. The largest values of $\tilde{h}_{10}$ are found in the North Atlantic, where the thermocline is deeper compared with other basins. Frontal regions, such as the Gulf Stream and the North Atlantic Current can also be identified from these fields. The XBT- and Argo-derived estimates of $\tilde{h}_{20}$ also show similar spatial patterns (Figure 4). Both XBT and Argo estimates capture the location of the subtropical gyres in the Pacific and South Atlantic and the east-west gradient of the depth of the 20°C isotherm in the equatorial oceans as well. The Argo-derived $\tilde{h}$ estimates are statistically significant over most of the global ocean. The XBT-derived $\tilde{h}$ are statistically significant in most regions, with the exception of subpolar oceans, the northeastern tropical Pacific and south Atlantic subtropical gyre where the density of observations is low.

Subtle differences are identified between the XBT- and Argo-derived pseudo-climatologies for the 10°C and 20°C isotherm depth. For instance, the pseudo-climatological 20°C isotherm is deeper in the center of the North Pacific subtropical gyre in the XBT-derived estimates (Figure 4). These differences are revealed when the respective climatologies are subtracted (Figure 5). A large fraction of the observed regions of the ocean show differences that are not statistically significant, especially in the Atlantic and Indian oceans. In regions where the difference can be estimated with 1-

sigma confidence, the differences between the estimates are mostly positive. This suggests a systematic depth bias in the XBTs compared with the Argo estimates, as Argo floats are assumed not to have systematic bias due to their higher accuracy in measuring depths. The differences are considered statistically significant when the 1-sigma confidence intervals of the XBT and Argo estimates do not overlap. The confidence intervals are obtained from the standard error of the $\widetilde{h}$ estimator, which amplitude is given by (6). The differences between estimates are not significant over large regions, such as the North Pacific and North Atlantic subtropical gyres. This could be related to larger variability in these regions and highlights the difficulty in identifying biases from the highly energetic mesoscale field. Nonetheless, the number of bins where the implied differences are statistically significant greatly exceeds the spatial coverage of previous studies (e.g. Hanawa et al. 1995; Gouretski and Koltermann 2007; Wijffels et al. 2008).

Differences in the values of ε^{-1}, a parameter related to the stratification, are also possible, but possibly restricted to higher order problems in the XBT FRE. Our analysis shows very few bins with statistically significant differences in the correlation gain (Figure 6). This is consistent with a FRE problem, since this type of error should not introduce changes in the stratification. However, other systematic errors, such a temperature bias, should not introduce biases in the estimation of the stratification as well.

Furthermore, the differences between the XBT minus Argo isotherm depths are larger for the 10°C isotherm (Figure 5a) compared with the 20°C isotherm (Figure 5b). Differences increasing with depth could be linked with a depth dependent bias between the two observing platforms. Globally, this depth dependence is clearly observed for all isotherms when the XBT minus Argo differences are analyzed as a function of isotherm depth (Figure 7). Most of the statistically significant differences are positive (red dots in Figure 7), indicating that XBT-derived pseudo climatologies are deeper than the Argo-derived estimates. Surprisingly, those differences that are not statistically significant (gray dots in Figure 7) fall inside the 2% errors bounds specified by Sippican (dashed-dot line in Figure 7). These XBT minus Argo differences (Figure 7) correspond to pseudo-climatology estimates obtained from regressions with correlation coefficients larger than 0.8, and that do not differ by more 0.1 between XBT and Argo. The depth dependent bias implied by the XBT minus Argo differences is independent of the correlations between isotherm depth and SHA; however, the differences between pseudo-climatologies from these high correlations show reduced scatter.

The following linear fits are obtained when the global depth dependent XBT minus Argo differences, Δh, are adjusted using a least-squares best-fit line with no offset at the ocean surface:

$$\Delta h_{XBT-Argo} = (0.030 \pm 0.002) \cdot h \qquad (7),$$

or with an offset at the surface:

$$\Delta h_{XBT-Argo} = (0.020 \pm 0.004)h + (4.7 \pm 1.3)m \quad (8).$$

The slope of these straight lines (solid and dashed lines in Figure 7, respectively) represents an estimate of a depth dependent error expressed as a percentage of the depth.

For instance, (7) indicates that XBTs overestimate the depths of the isotherms with respect to Argo depths by (3.0±0.2)% in the global ocean. The offset in (8) indicates that XBTs overestimate the isotherm depths by (4.7±1.3) m plus a (2.0±0.4)% of the Argo depths. The uncertainty in the coefficients corresponds to the 1-sigma confidence intervals obtained from the least-squares fit. The implications of these results for detecting problems in the FRE are discussed in the following section. The slope and offset for the least-squares lines show values ranging from 0.1 % to 3.7% and from 0.1 m to 11.4 m respectively in different ocean basins and depending on the type of equation used to fit the differences (Table 1; Figure 8). Both lines fall outside the 2% error envelope specified by Sippican in all ocean basins (dashed-dot line in Figures 7 and 8).

Discussion

Our analysis of XBT and Argo observations for the 2000-2007 period provides evidence for a depth dependent bias consistent with an error in the FRE equation. The positive XBT minus Argo differences indicate that XBTs are actually falling slower than the specified terminal velocity in the H95-corrected FRE equation. The implied bias results in XBT depths that are too deep, therefore producing a warm temperature bias that increases with depths throughout most of the water column. The error associated with this bias is estimated from the slope of the least-squares fit of the XBT minus Argo differences (7):

$$\gamma_1 = \frac{z_{H95} - z_{Argo}}{z_{Argo}} = 0.030 \pm 0.002\,, \qquad (9)$$

where z_{H95} is the H95-corrected XBT depth, and z_{Argo} is considered here to be the true depth. This depth-dependent error allows correction of z_{H95} as follows:

$$z_{Argo} = \frac{1}{(1+\gamma_1)} z_{H95} \qquad (10).$$

The global correction factor $(1+\gamma_1)^{-1}$ of 0.97 in (10) is approximately the inverse of the stretching factor f_{H95} = 1.0336, implemented after the H95 study. This strongly suggests that the H95 correction could have introduced the bias during the 2000-2007 period.

The conclusion presented above is consistent with the analysis of Wijffels et al. (2008), which showed that since 2000, XBTs are falling with a terminal velocity close to the original Sippican values. Their comparison of CTD and XBT data showed that the H95 study was done at a time when the terminal velocity (represented by the *b* coefficient in the FRE) was faster than at any other time. This return of the terminal velocity values back to the original Sippican values has been independently confirmed by field intercomparisons (D. Snowden, personal communication). Our study not only confirms the value of the FRE bias, but also provides evidence of its global extent, since we identify approximately the same error in the H95-corrected XBT depths in all ocean basins, with the exception of the North Pacific (Table 1). The apparent global extent of the bias points to problems in the XBT instruments rather than the influence of regional differences in ocean conditions, such as the effect of temperature on the hydrodynamic drag.

Additionally, an offset at the surface is identified when the XBT minus Argo differences are fitted using a straight line with a constant term (8). Both XBT and Argo are unable to observe the upper few meters of the water column with precision. However surface offsets are still detectable because any systematic bias introduced in the initial seconds of the XBT descent results in a vertical shift of the entire temperature profile. The depth-dependent error, γ_2, and offset, δ_2, obtained from the least-squares fit allows to correct z_{H95} as follows:

$$z_{Argo} = \frac{1}{(1+\gamma_2)}(z_{H95} - \delta_2) \qquad (11).$$

The values obtained for the γ_2 and δ_2 coefficients show more disparity between the different ocean basins (Table 1) compared with the γ_1 coefficient in correction (10). Overall, the values of the δ_2 offset are consistent with values reported by previous studies of 3.7 m (Bailey et al. 1989;), 4.2 m (Singer 1990), 2 to 10m (Kizu and Hanawa 2002), 2 m (Reseghetti et al. 2007), and 4.5 m (D. Snowden, personal communication).

Surface offsets have received a great deal of attention and have been attributed to a wide range of transients resulting from the thermistor response, the recording system, or the hydrodynamics of the descent of the probe (Green 1984; Roemmich and Cornuelle 1987; Hallock and Teague 1992; Kizu and Hanawa 2002; Reseghetti et al. 2007). Sippican recommends launching XBTs from a height *H*, of about 2.5 m to ensure that the entry speed is $\sqrt{2gH} \sim 6.5ms^{-1}$, equal to the terminal speed, and thus avoid hydrodynamical transients. In other words, the FRE assumes that the probe starts the descent with the terminal velocity implied by the *b* coefficient. The entry speed is expected to be much larger for XBTs launched from cargo ships, because they are typically dropped from the stern or the bridge, which are several meters above the ocean surface. An initial velocity larger than the terminal velocity represents a faster *b* coefficient during the initial decent and results in a negative offset at the surface. In contrast, the *positive* 4.7 m offset suggested by our analysis is consistent with a probe descending with an initial velocity closer to zero (Hallock and Teague 1992, Table 1), thus unlikely to result from hydrodynamic transients.

A positive offset could also result from the finite time response of the temperature sensor to sudden changes in temperature, which typically occur when the probe enters the ocean and when it crosses the base of the mixed layer (e.g. Roemmich and Cornuelle 1987; Kizu and Hanawa 2002; Reseghetti et al. 2007). Different recording systems are used in the different ocean basins, thus explaining why we find different values. However, a comparison of the different acquisition systems (SEAS2000, Devil, Sippican) indicates that they exhibit approximately the same offset (D. Snowden, personal communication). In contrast, our analysis shows that considering a surface offset in the least-squares fit of the XBT minus Argo differences leads to less robust estimates of depth error, γ, and surface offset, δ (Table 1, columns 3 and 4). Briefly stated, the only robust bias detected from our analysis is a 3% depth dependent error, with no evidence for a robust surface offset. Addressing this problem is important because this surface offset could introduce biases of up to 10% when estimating the depth of shallow mixed layers becoming an important source of error. More research is needed to determine its origin, and whether it is introduced when probe enters the ocean or when the probe crosses the mixed layer.

Conclusions

A methodology is proposed to estimate climatologies of isotherm depths using a combination of *in situ* and satellite observations. The methodology allows the estimation of climatologies for relatively short periods reducing sampling problems by using correlations with satellite-derived SHA fields. This represents an important advantage compared with the analysis of nearby XBT/CTD, which is difficult to perform on a global scale, and that has been the main methodology for identifying and characterizing these biases up to date. Moreover, this methodology overcomes limitations in comparing XBTs with in-situ hydrography directly, which require very large amounts of data to be able to detect biases obscured by the highly energetic mesoscale field. The methodology presented here avoids these limitations by taking advantage of the high temporal and spatial resolution of satellite altimetry observations.

Comparison of XBT and Argo estimates of isotherm depth suggests a depth dependent bias in XBT observations in all regions of the world ocean, which confirms the global extent of a depth dependent error in the XBTs reported in previous studies (Gouretski and Koltermann 2007; Wijffels et al. 2008). Moreover, our results show that this error can be identified with 1-sigma statistical significance despite the inhomogeneous sampling of the eddy variability by Argo and XBTs. The 3% depth error identified here is also suggestive of a time-dependent bias in the XBTs, since it appears that the H95 correction is no longer appropriate for current XBTs. This indicates that the original FRE coefficients specified by Sippican would be adequate for the 2000-2007 period. The source of the time-dependent FRE bias remains unclear. However, the global extent of the implied bias points to problems in the instrumentation, such as changes in the terminal velocity of the XBTs, which are likely to result from variations in the drag characteristics of the probes. The robust global extent of the bias points to problems in the XBT instruments rather than the influence of regional differences in ocean conditions. While there are several potential sources of near-surface errors due to transients in the descent of the probe, our study shows that surface offsets are different among ocean basins, thus unable to be explained by a systematic problem in the XBT FRE. According to our results, returning to the original FRE coefficients is the only correction that seems to be robust. This correction could bring the XBT dataset to consistency with Argo during the 2000-2007 period.

XBTs remain the second most important source of upper ocean thermal data and the most important source of temperature along transects. The FRE coefficients need to be monitored on a continuous basis to identify future changes in the terminal velocity of the XBT, which may avoid introducing spurious decadal signals in global heat storage. The methodology presented here is especially well suited for this purpose because it allows the comparison of XBT and Argo data over relatively short periods. High-density transects, which are run four times per year, could provide the number of observations to perform this type analysis over one or two year periods. Additionally, these transects must coincide with regions of high density of Argo observations, such as the North Pacific or the North Atlantic.

Acknowledgements

Argo data were collected and made freely available by Argo (a pilot program of the Global Ocean Observing System) and contributing national programs (http://www.argo.net/). The altimeter products were produced by Ssalto/Duacs and distributed by AVISO, with support from CNES. We thank to all the scientists, technicians, and crewmembers of ships of opportunity that contribute to the collection of XBT and Argo observations around the world. We thank Claudia Schmid for providing the quality controlled CTD, Argo, and XBT profiles. This research was carried out in part under the auspices of CIMAS, a join institute of the University of Miami and NOAA (Cooperative Agreement NA17RJ1226). We are grateful to Molly Baringer, Ann Thresher, Viktor Gouretski, Robert Molinari, Joshua Willis, and two anonymous reviewers for insightful comments that helped improved the study. The NOAA Climate Program Office funded this work.

References

Bailey, R., H. Phillips, and G. Meyers, 1989: Relevance to TOGA of systematic XBTerrors. In: Picaut, J., Lukas, R. (Eds.), Proceedings of the Western Pacific International Meeting and Workshop on TOGA COARE, Noumea, pp. 775–784.

Conkright, M. E., R. Locarnini, H. Garcia, T. O'Brien, T. P. Boyer, C. Stephens, and J. Antonov, 2002: World Ocean Atlas 2001 Objective Analyses, Data Statistics and Figures. National Oceanographic Data Center, Silver Spring, MD, CD-ROM, Data Set Doc., 17 pp.

Fedorov, K. N., A. I. Ginzburg, and A. G. Zatsepen, 1978: Systematic differences in isotherm depths derived from XBT and CTD data. *POLYMODE News*, **50**(1), 6–7.

Flierl, G. and A. R. Robinson, 1977: XBT measurements of the thermal gradient in the MODE eddy. *J. Phys. Oceanogr.*, **7**, 300–302.

Gilson, J., D. Roemmich, B. Cornuelle, and L.-L. Fu, 1998: Relationship of TOPEX/Poseidon altimetric height to steric height and circulation of the North Pacific. *J. Geophys. Res.*, **103**, 27,947–27,965.

Goni, G., S. Kamholz, S. Garzoli, and D. Olson, 1996: Dynamics of the Brazil-Malvinas Confluence based on inverted echo sounders and altimetry. *J. Geophys. Res.*, **101**(C7), 16,273–16,289.

Gouretski, V. V., and K. P. Koltermann, 2007: How much is the ocean really warming? *Geophys. Res. Lett.*, **34**, L01610, doi:10.1029/2006GL027834.

Green A. W., 1984: *Bulk dynamics* of the *expendable bathythermograph* (XBT). *Deep-Sea Res.*, **31**, 415–483.

Hallock, Z. R. and W. J. Teague, 1992: The fall rate of the T-7 XBT. *J. Atmos. Oceanic Technol.*, **9**, 470–483.

Hanawa, K., P. Rual, R. Bailey, A. Sy, and M. Szabados, 1995: A new depth-time equation for Sippican or TSK T-7, T-6 and T-4 expendable bathythermographs (XBT). *Deep Sea Res. I*, **42**, 1423–1451.

Kizu, S. and K. Hanawa, 2002: Start-up transient of XBT measurement. *Deep-Sea Res. Part I*, **49**, 935–940.

Lawson, C. and R. Hanson. Solving Least Squares Problems. *Prentice-Hall.*

Le Traon, PY, F. Nadal and N. Ducet, 1998: An Improved Mapping Method of Multi-Satellite Altimeter Data. *J. Atmos Ocean Tech*, **25**, 522–534.

Levitus, S., J. I. Antonov, T. P. Boyer, R. A. Locarnini, H. E. Garcia, and A. V. Mishonov, 2009: Global ocean heat content 1955–2008 in light of recently revealed instrumentation problems. *Geophys. Res. Lett.,* **36**, L07608.

Mayer D., R. Molinari, M. Baringer, and G. Goni, 2001: Transition regions and their role in the relationship between sea surface height and subsurface temperature structure in the Atlantic Ocean. *Geophys. Res. Let*., **28,** 3943-3946.

McDowell, S., 1977: A note on XBT accuracy. *POLYMODE News*, **29**(1), 4–8.

Reseghetti, F., M. Borghini, and G. M. R. Manzella, 2007: Factors affecting the quality of XBT data – results of analyses on profiles from the Western Mediterranean Sea. *Ocean Sci.*, **3**, 59–75.

Roemmich, D. and B. Cornuelle, 1987: Digitization and calibration of the expendable bathythermograph. *Deep-Sea Res.*, **34**, 299–307.

Roemmich, D. and J. Gilson, 2001. Eddy transport of heat and thermocline waters in the North Pacific: A key to interannual/decadal climate variability. *J. Phys. Oceanogr.*, **31**, 675-687.

Saunders, P. M., 1981: Practical conversion of pressure to depth. *J. Phys. Oceanogr.*, **11**(4), 573–574.

Schmid, C., 2005: Impact of Combining Temperature Profiles from Different Instruments on an Analysis of Mixed Layer Properties. *J. Atmos. Oceanic Technol.*, **22**(10), 1571–1587.

Seaver, G. A., and S. Kuleshov, 1982: Experimental and analytical error of expendable bathythermograph. *J. Phys. Oceanogr.*, **12**, 592–600.

Singer, J., 1990: On the error observed in electronically digitized T7 XBT data. *J. Atmos. Oceanic Technol.*, **7**, 603–611.

Wijffels, S. E., J. Willis, C. M. Domingues, P. Barker, N. J. White, A. Gronell, K. Ridgway, and J. A. Church, 2008: Changing Expendable Bathythermograph Fall Rates and Their Impact on Estimates of Thermosteric Sea Level Rise. *J. Climate*, **21**, 5657–5672.

Willis, J. K., J. M. Lyman, G. C. Johnson, and J. Gilson, 2009: In Situ Data Biases and Recent Ocean Heat Content Variability. *J. Atmos. Oceanic Technol.*, 26, 846–852.

Willis, J. K., D. Roemmich, and B. Cornuelle, 2004: Interannual variability in upper ocean heat content, temperature, and thermosteric expansion on global scales. *J. Geophys. Res.*, **109**, C12036, doi:10.1029/2003JC002260.

Figure list

Figure 1 – Correlation coefficient between the altimetry-derived SHA and the depth of the 10°C isotherm (h_{10}) from (a) Argo and (b) XBT profiles. Correlation coefficient between the altimetry-derived SHA and the depth of the 20°C isotherm (h_{20}) from (c) Argo and (d) XBT profiles. Stippling indicates regions where the correlation coefficients are not significant with 67% confidence based on a chi-squared test. The correlation coefficients between the Argo-derived isotherm depth and altimetry-derived SHA are significant over most of the global ocean. The correlation coefficients between XBT-derived isotherm depth and altimetry-derived SHA are significant over the major shipping lines coinciding where the density of observations is largest...............................37

Figure 2 – (a) Dispersion diagram between in-situ observations of the depth of the 20°C isotherm (h_{20}) and concurrent estimates of satellite-derived sea height anomaly (η') in a 3°×3° bin centered at 169°W 4°S. (b) Dispersion diagram between in-situ observations of the depth of the 10°C isotherm (h_{10}) and concurrent estimates of satellite-derived sea height anomaly (η') in a 3°×3° bin centered at 175°W 25°S. Gray diamonds and black circles correspond to the XBT-derived and Argo-derived estimates of isotherm depth respectively. The blue and the red lines are the least-squares best-fit line between the satellite-derived sea height anomaly and the XBT-derived and Argo-derived isotherm depth estimates respectively. Note that the y-axis is inverted so deeper isotherm depths appear on the bottom of the scatter plot.........38

Figure 3 – Pseudo-climatologies of the depth of 10°C isotherm $\tilde{h}_{10}$, computed following the methodology described in the text using (a) Argo and (b) XBT temperature profiles. The $\tilde{h}_{10}$ estimates are computed on 3°×3° bins using XBT or Argo data from 2000 to 2007

combined with altimetry–derived sea height anomaly fields. Stippling indicates regions where $\widetilde{h}_{10}$ is not significant with 67% confidence, which in general coincides with regions where the density of observations is low. 39

Figure 4 – Pseudo-climatologies corresponding to the 20°C isotherm computed following the methodology described in the text using (a) Argo and (b) XBT temperature profiles combined with altimetry-derived sea height anomaly fields. See Figure 3 for more details. 40

Figure 5 – XBT minus Argo difference of the pseudo climatologies of the depth of the (a) 10°C isotherm and the (b) 20°C isotherm. Positive values indicate deeper XBT-derived isotherm depths. The pseudo-climatologies correspond to the 2000 to 2007 period and are computed using XBT or Argo data combined with altimetry-derived sea height anomalies as described in the text. Stippling indicates regions where the difference between the estimates is not significant with 67% confidence. 41

Figure 6 – XBT minus Argo difference in regression gain of the depth of the (a) 10°C and the (b) 20°C isotherms. Stippling indicates regions where the difference between the estimates is not significant with 67% confidence..42

Figure 7 – Scatter plot of the differences between the pseudo-climatological isotherm depth estimates as a function of depth for the global ocean. The depth axis corresponds to the pseudo-climatological isotherm depth derived from Argo. Positive $h_{XBT} - h_{Argo}$ differences indicate that the XBT estimates result in deeper isotherms for the period 2000–2007. Only pseudo-climatologies obtained from regressions with correlation coefficients larger than 0.8 and with a difference of less than 0.1 between XBTs and Argo are shown. Red dots

correspond to 1-sigma significant biases while gray dots are not significant with the same confidence level. The dashed-dot lines indicate the 2% error bounds specified by the manufacturer. The solid dashed line corresponds to the least–squares fit allowing for an offset at the surface while the solid line is adjusted with no offset at the surface. 43

Figure 8 – Scatter plot of the differences between the pseudo-climatological isotherm depth estimates as a function of depth for different regions: (a) North Atlantic, (b) South Atlantic, (c) North Pacific, (d) South Pacific, (e) Tropical Pacific, and (f) Indian oceans. See Figure 8 for more details. 44

Table list

	$\Delta h_{\text{XBT-Argo}} = \gamma_1 z$	$\Delta h_{\text{XBT-Argo}} = \gamma_2 z + \delta_2$	
	γ_1 (%)	γ_2 (%)	δ_2 (m)
Global	3.0 ± 0.2	2.0 ± 0.4	4.7 ± 1.3
North Atlantic	2.6 ± 0.2	2.6 ± 0.5	0.1 ± 1.1
South Atlantic	3.7 ± 0.3	1.1 ± 0.6	11.4 ± 1.6
North Pacific	2.2 ± 0.3	1.7 ± 0.5	2.3 ± 1.3.
South Pacific	3.2 ± 0.3	2.4 ± 0.6	2.6 ± 1.9
Tropical Pacific	3.6 ± 0.5	0.1 ± 1.0	8.1 ± 1.5
Indian Ocean	3.0 ± 0.3	2.0 ± 0.7	4.8 ± 2.9

Table 1 – Corrections to the fall-rate equation obtained from least-squares fitting of the XBT minus Argo differences as a function of depth obtained in this study. The uncertainty in the coefficients corresponds to the 1-sigma confidence intervals obtained from the least-squares fit.

Figures

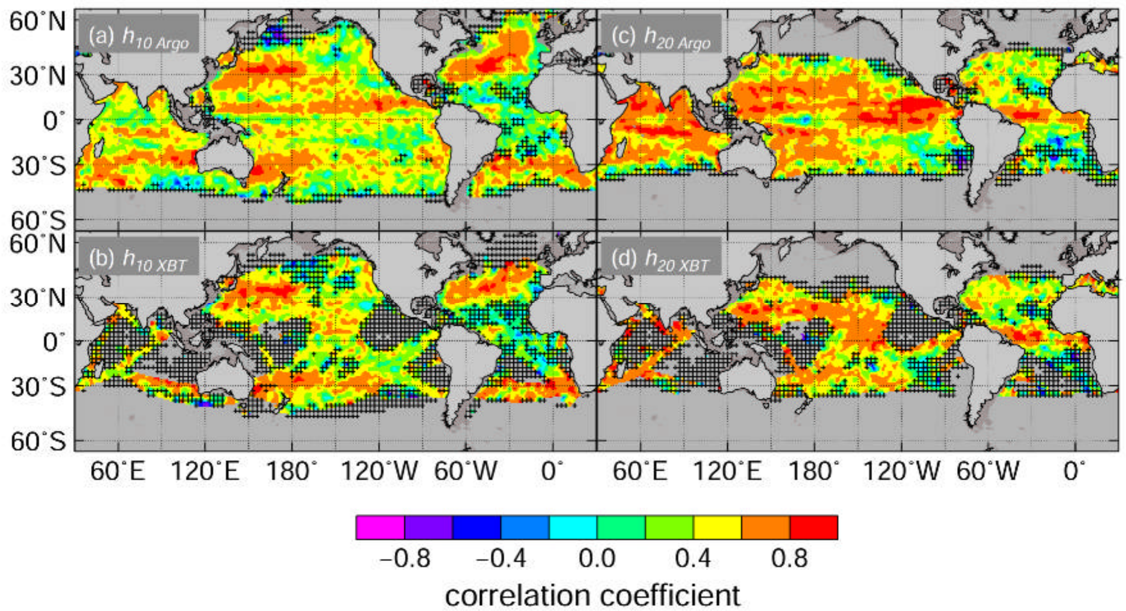

Figure 1 – Correlation coefficient between the altimetry-derived SHA and the depth of the 10°C isotherm (h_{10}) from (a) Argo and (b) XBT profiles. Correlation coefficient between the altimetry-derived SHA and the depth of the 20°C isotherm (h_{20}) from (c) Argo and (d) XBT profiles. Stippling indicates regions where the correlation coefficients are not significant with 67% confidence based on a chi-squared test. The correlation coefficients between the Argo-derived isotherm depth and altimetry-derived SHA are significant over most of the global ocean. The correlation coefficients between XBT-derived isotherm depth and altimetry-derived SHA are significant over the major shipping lines coinciding where the density of observations is largest.

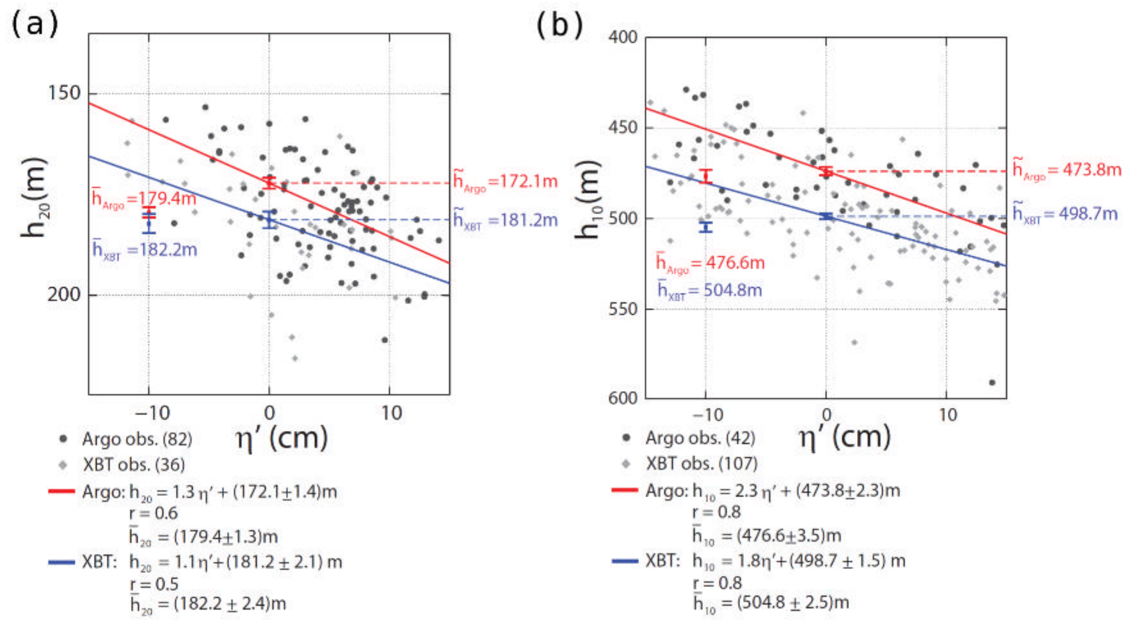

Figure 2 – (a) Dispersion diagram between in-situ observations of the depth of the 20°C isotherm (h_{20}) and concurrent estimates of satellite-derived sea height anomaly (η') in a 3°×3° bin centered at 169°W 4°S. (b) Dispersion diagram between in-situ observations of the depth of the 10°C isotherm (h_{10}) and concurrent estimates of satellite-derived sea height anomaly (η') in a 3°×3° bin centered at 175°W 25°S. Gray diamonds and black circles correspond to the XBT-derived and Argo-derived estimates of isotherm depth respectively. The blue and the red lines are the least-squares best-fit line between the satellite-derived sea height anomaly and the XBT-derived and Argo-derived isotherm depth estimates respectively. Note that the y-axis is inverted so deeper isotherm depths appear on the bottom of the scatter plot.

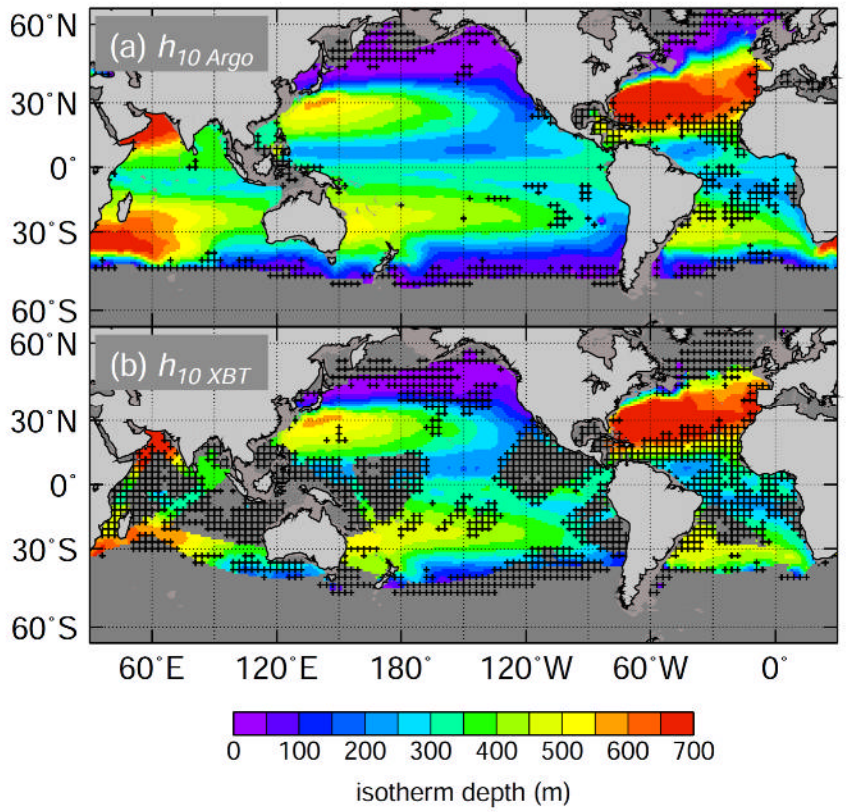

Figure 3 – Pseudo-climatologies of the depth of 10°C isotherm $\widetilde{h}_{10}$, computed following the methodology described in the text using (a) Argo and (b) XBT temperature profiles. The $\widetilde{h}_{10}$ estimates are computed on 3°×3° bins using XBT or Argo data from 2000 to 2007 combined with altimetry–derived sea height anomaly fields. Stippling indicates regions where $\widetilde{h}_{10}$ is not significant with 67% confidence, which in general coincides with regions where the density of observations is low.

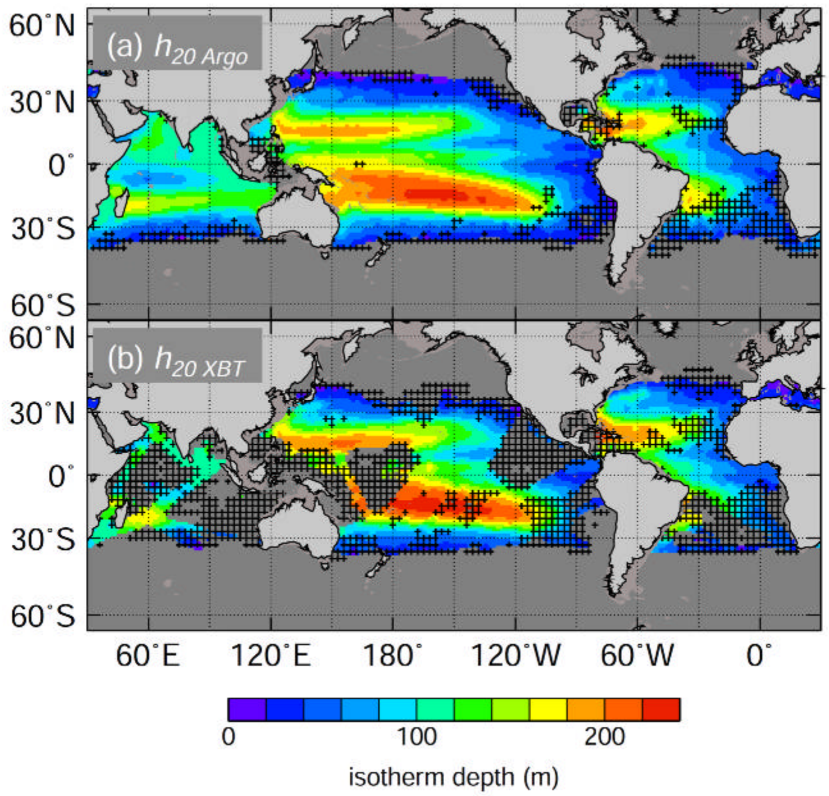

Figure 4 – Pseudo-climatologies corresponding to the 20°C isotherm computed following the methodology described in the text using (a) Argo and (b) XBT temperature profiles combined with altimetry-derived sea height anomaly fields. See Figure 3 for more details.

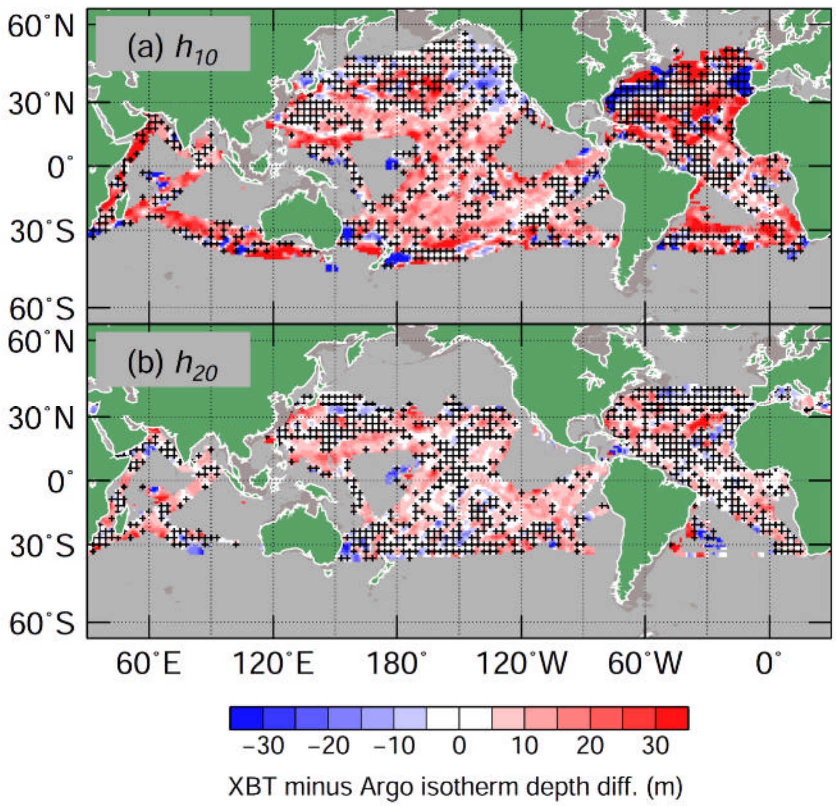

Figure 5 – XBT minus Argo difference of the pseudo climatologies of the depth of the (a) 10°C isotherm and the (b) 20°C isotherm. Positive values indicate deeper XBT-derived isotherm depths. The pseudo-climatologies correspond to the 2000 to 2007 period and are computed using XBT or Argo data combined with altimetry-derived sea height anomalies as described in the text. Stippling indicates regions where the difference between the estimates is not significant with 67% confidence.

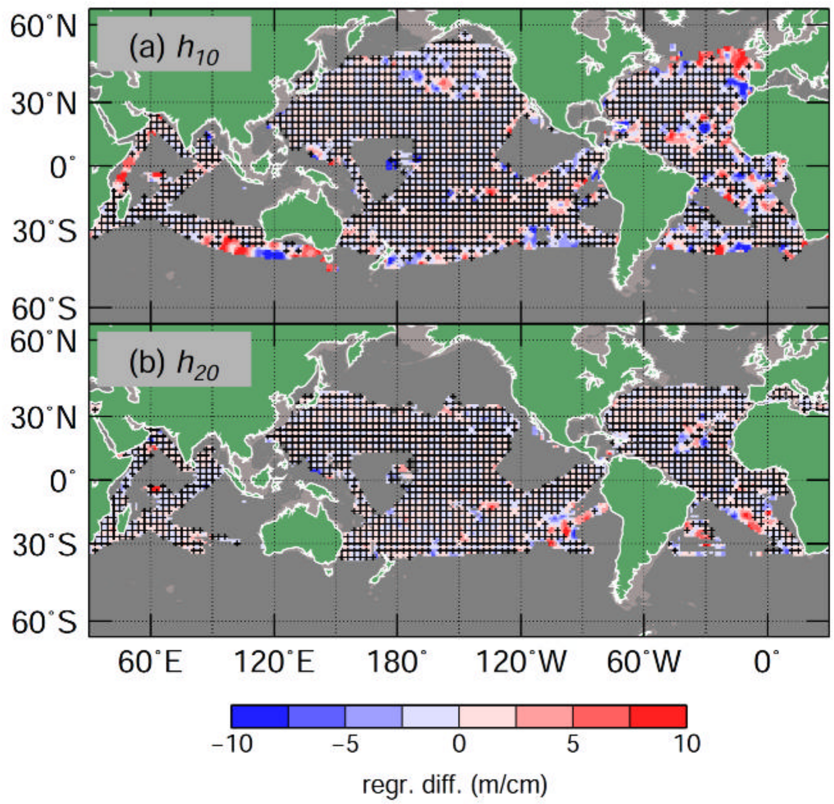

Figure 6 – XBT minus Argo difference in regression gain of the depth of the (a) 10°C and the (b) 20°C isotherms. Stippling indicates regions where the difference between the estimates is not significant with 67% confidence.

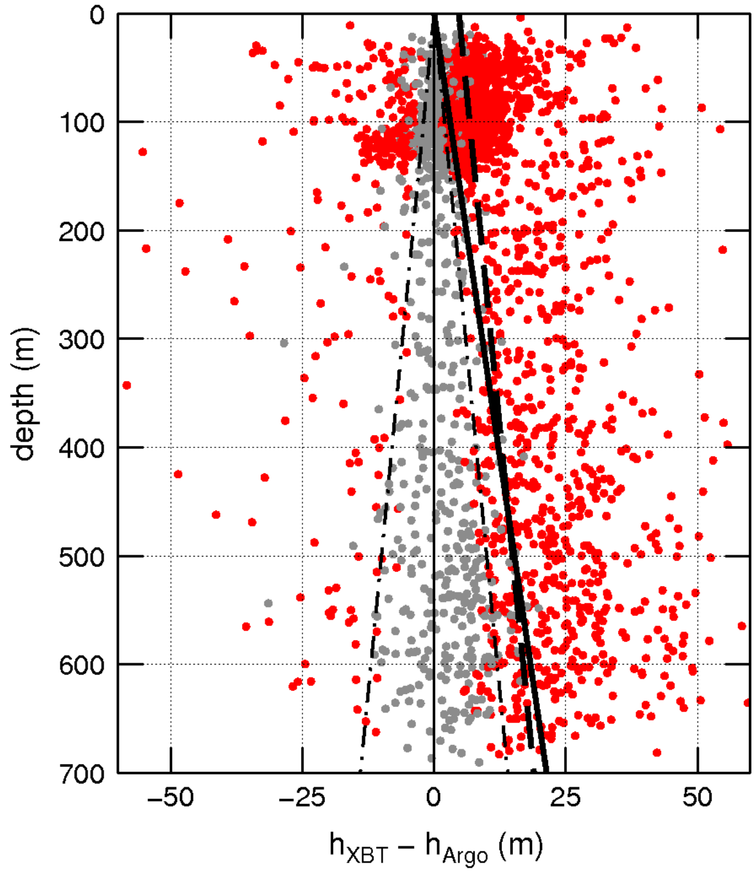

Figure 7 – Scatter plot of the differences between the pseudo-climatological isotherm depth estimates as a function of depth for the global ocean. The depth axis corresponds to the pseudo-climatological isotherm depth derived from Argo. Positive $h_{XBT} - h_{Argo}$ differences indicate that the XBT estimates result in deeper isotherms for the period 2000–2007. Only pseudo-climatologies obtained from regressions with correlation coefficients larger than 0.8 and with a difference of less than 0.1 between XBTs and Argo are shown. Red dots correspond to 1-sigma significant biases while gray dots are not significant with the same confidence level. The dashed-dot lines indicate the 2% error bounds specified by the manufacturer. The solid dashed line corresponds to the least–squares fit allowing for an offset at the surface while the solid line is adjusted with no offset at the surface.

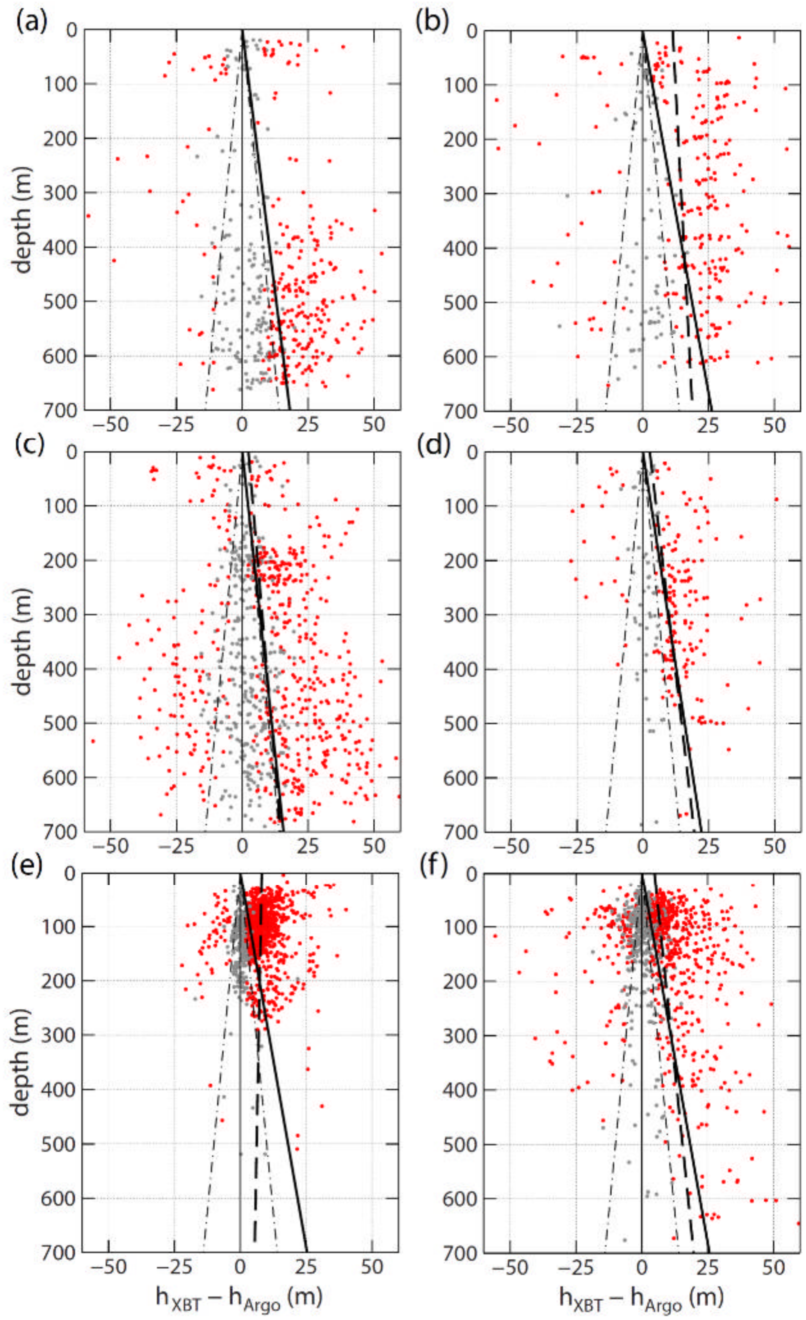

Figure 8 – Scatter plot of the differences between the pseudo-climatological isotherm depth estimates as a function of depth for different regions: (a) North Atlantic, (b) South Atlantic, (c) North Pacific, (d) South Pacific, (e) Tropical Pacific, and (f) Indian oceans. See Figure 8 for more details.